JOURNAL OF MOLECULAR SPECTROSCOPY **161**, 312–316 (1993)

NOTE

Electric-Resonance Optothermal Spectrum of the $K_a = 1 \leftarrow 0$ Band of DHO–DOD: Direct Observation of the $1 \rightarrow 4$ Tunneling Splitting

Recently, we have reported (*1*) the observation of the electric-resonance optothermal spectrum of the $K_a = 1 \leftarrow 0$ rotation-tunneling band of $(D_2O)_2$. In the present note we report the extension of these measurements to the $K_a = 1 \leftarrow 0$ band of DHO–DOD, where the DHO unit is the proton acceptor.

Although, the microwave and far-infrared spectra of $(H_2O)_2$ and $(D_2O)_2$ have been extensively studied (for a review, see (*2*)), little is known about the rotation-tunneling splittings in the mixed D/H dimers (*3, 4*). The investigation of these mixed isotopic species will provide further insight into the complicated dynamics exhibited in the water dimer. For example, isotopic substitution allows us to examine the mass dependence of the observed tunneling splittings to furnish information about the kinetic energy operator for the various tunneling pathways. Also, because of the symmetry reduction realized in the mixed isotopic species, the rotation-tunneling selection rules are relaxed, allowing, in the case of DHO–DOD studied here, the direct measurement of the $1 \rightarrow 4$ tunneling splitting, the largest of the tunneling splittings in the dimer. For $(D_2O)_2$ and $(H_2O)_2$, this splitting has to be inferred from a fitting of the observed spectrum to an assumed model Hamiltonian.

The present measurements were made using an electric-resonance optothermal spectrometer described previously in our investigation of $(H_2O)_2$ (*5, 6*) and $(D_2O)_2$ (*1, 7, 8*).[1] In Fig. 1 we present an energy level diagram for DHO–DOD illustrating the four symmetry allowed $K_a = 1 \leftarrow 0$ subbands. Figure 2 shows a spectrum of one of the two $K_a = 1 \leftarrow 0$ Q branches observed. The individual J transitions appear as doublets with a 2:1 intensity ratio resulting from a tunneling motion which interchanges the two deuterons on the proton-donor subunit. The observed $K_a = 1 \leftarrow 0$ transitions are summarized in Table I. Both b- and c-type transitions are observed originating from a common $K_a = 0$ lower state, as inferred from the essentially identical $\bar{B}_{K=0}$ values determined in the fitting of the individual subbands to the frequency expression

$$\nu = \nu_0 + \bar{B}_{K=1}[J'(J'+1) - K_a'^2] - D_{K=1}[J'(J'+1) - K_a'^2]^2 + (-1)^{K_a'+K_c'+J'}\frac{(B-C)_{K=1}}{4}J'(J'+1) - \bar{B}_{K=0}J''(J''+1) + D_{K=0}J''(J''+1), \quad (1)$$

where $\bar{B} = (B + C)/2$.

The spectroscopic constants determined from these fits are listed in Table II. In the final fits we have constrained the $\bar{B}_{K=0}$ values for the b-type bands to the values determined for the more extensively characterized c-type bands. Note that the determined $\bar{B}_{K=0}$ and $D_{K=0}$ values are similar to, but different from, the $\bar{B}_{K=0} = 5648.274$ MHz and $D_{K=0} = 0.0407$ MHz values determined by previous microwave studies (*3, 4*) on the lowest energy ground $K = 0$ A/B states of Fig. 1. This leads us to assign the present transitions as originating from the upper $K = 0$ state. These transitions are shown as solid lines in Fig. 1. No $K = 1 \leftarrow 0$ microwave lines were observed for the ground $K = 0$ states (shown as dashed lines in Fig. 1) since these transitions are expected to be too high in frequency for the microwave sources used here.

In the case of both $(H_2O)_2$ and $(D_2O)_2$ the equilibrium plane of symmetry allows only the observation of the c-type $K = 1 \leftarrow 0$ band.[2] However, for the DHO–DOD dimer this symmetry plane no longer exists so that both b- and c-type transitions are observed. As seen in Fig. 1, the 43-GHz separation between the origins of the b-type and the origins of the c-type subbands directly furnishes the $1 \rightarrow 4$ methylamine-type tunneling matrix element for the $K_a = 1$ state of the dimer as $|h_{4v}| = 10.7$ GHz. In the case of both $(D_2O)_2$ and $(H_2O)_2$ the presence of only the c-type $K = 1 \leftarrow 0$ transitions prevents a direct determination of the

[1] Typographical errors exist in Table I of Ref. (*7*). The transitions at 66313.13, 64000.45, and 74852.29 MHz should be labeled as $B_1^+\ 6_{06} \leftarrow 5_{05}$, $A_1^+\ 6_{06} \leftarrow 5_{05}$, and $B_1^+\ 7_{07} \leftarrow 6_{06}$, respectively.

[2] Group theoretically, transitions between the E_1 and E_2 states are also allowed; however, the intensities for these transitions are expected to be small except in the near free-rotor limit where the interchange tunneling splitting is large.

0022-2852/93 $5.00

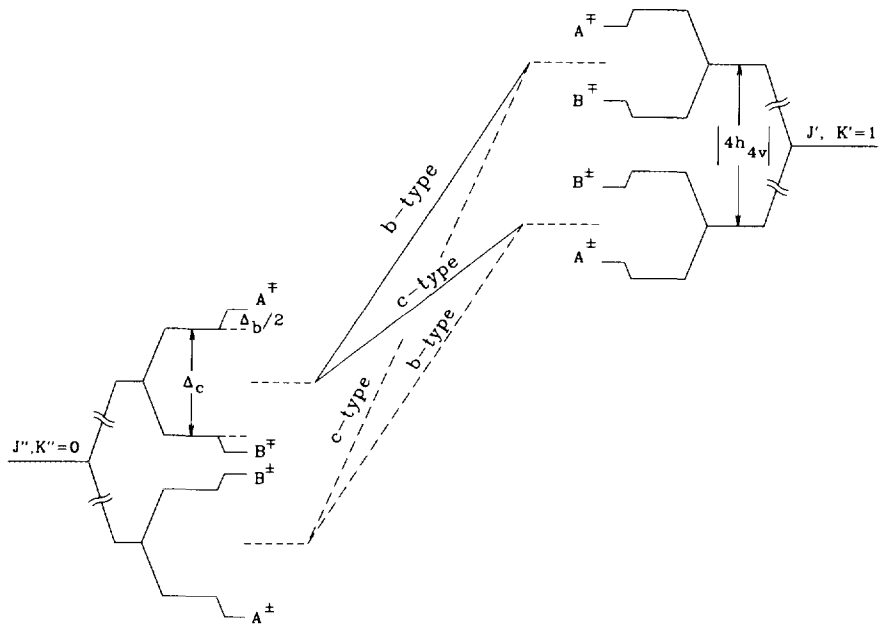

FIG. 1. Energy-level diagram for DHO–DOD. The observed $K = 1 \leftarrow 0$ bands are designated by solid lines. For the $K = 1$ state only one asymmetry component is shown. Every $J_{K_aK_c}$ state is split into A^+, A^-, B^+, and B^- state by tunneling. For the O_{00} state, the energy ordering from lower to higher energies is A^+, B^+, B^-, and A^-. The correct + or − parity choice for the other states is obtained from consideration of the $+ \leftrightarrow -$ parity selections rules for an electric dipole allowed transition.

h_{4v} matrix element. However, the average of the $K = 0$ and 1 tunneling matrix elements for the $1 \rightarrow 4$ motion in $(D_2O)_2$ has been determined as 8.9 GHz, and model calculations (*9*) give the $|h_{4v}|$ matrix element in $(H_2O)_2$ as 47.4 GHz.

The splitting of the $I_D = 1$, B symmetry, rotation-tunneling states from the $I_D = 0$, 2, A symmetry, rotation-tunneling states gives information about the tunneling process interchanging the two deuterons on the donor. Here, I_D is the resultant deuteron nuclear-spin function of the proton-donor unit. From consideration of $(D_2O)_2$ and $(H_2O)_2$, three possible tunneling pathways seem possible for the deuteron interchange motion and are pictured in Fig. 3. Pathway A corresponds to 180° rotation of the donor unit about its C_2 symmetry axis (*b*-inertial axis), pathway B has a bifurcated transition state which is obtained by simultaneous partial rotations of the donor about its *c*-inertial axis and the acceptor about its *a*-inertial axis, and pathway C is similar to the geared interconversion tunneling process in $(H_2O)_2$ and $(D_2O)_2$ which interchanges the donor and acceptor units. In DHO–DOD, the position along pathway C where the donor and acceptor roles are interchanged is an intermediate step in the deuteron interchange tunneling.

The rotation-tunneling state selection rules for the three possible tunneling processes differ. For A, the μ_b and μ_c dipole moment components of the complex are symmetric functions of the tunneling coordinate; for B, μ_b is symmetric and μ_c is antisymmetric; and for C, μ_b is antisymmetric and μ_c is symmetric. For μ_i symmetric, the "*i*-type" transitions do not change tunneling state, having selection rules symmetric $\leftrightarrow$ symmetric and antisymmetric $\leftrightarrow$ antisymmetric in the tunneling state. When μ_i is antisymmetric, the *i*-type selection rules are symmetric $\leftrightarrow$ antisymmetric in the tunneling state.

The observed splittings of $2\Delta_b = 9.2$ MHz for the *b*-type band and $2\Delta_c = 22.0$ MHz for the *c*-type band are thus inconsistent with a single tunneling pathway unless we invoke a large K_a and $1 \rightarrow 4$ tunneling state dependence to the deuteron interchange tunneling splitting. We note that in the case of the $(D_2O)_2$ dimer the tunneling splitting associated with pathway B is ~14 MHz and varies by less than 10% between K_a and $1 \rightarrow 4$ tunneling state. Because of the smaller reduced mass for pathway B in DHO–D_2O compared to that in D_2O–D_2O, we expect the B tunneling splitting to be larger than 14 MHz for the DHO–D_2O system. With these considerations, one explanation for the observed splittings is that both pathways B and C are important,

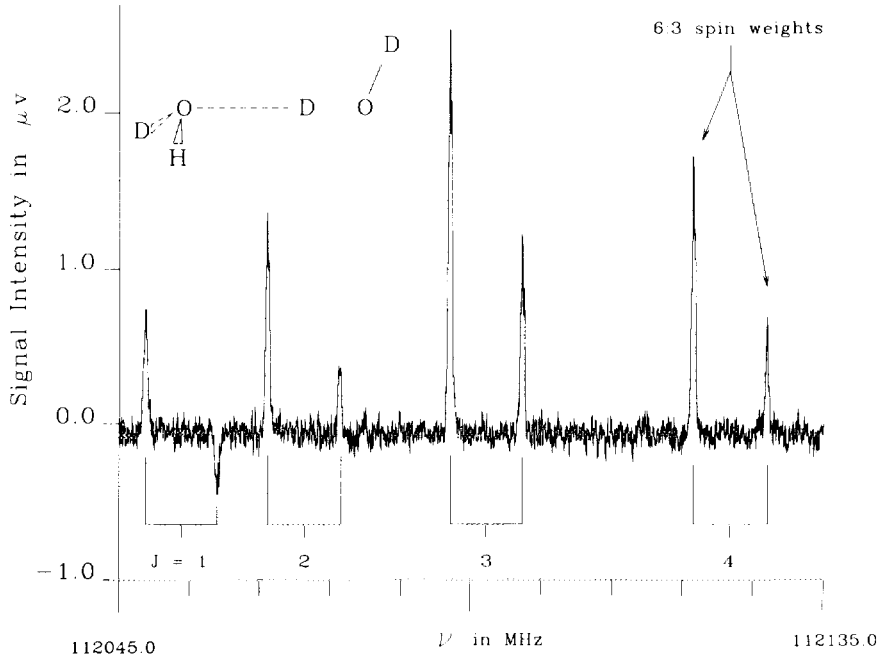

FIG. 2. Sample Q-branch spectrum of the b-type $K = 1 \leftarrow 0$ band of DHO–DOD showing the 2:1 intensity alternation arising from a tunneling motion which interchanges the two deuterons on the proton-donor unit.

TABLE I

Observed Transition Frequencies (in MHz) for the $K_a = 1 \leftarrow 0$ Rotation-Tunneling Bands of DHO–DOD

	b-type[a]		c-type	
	$A^{\pm}$[b]	$B^{\pm}$	$A^{\pm}$	$B^{\pm}$
g_I	6	3	6	3
P(3)	78143.63	78152.56	35289.44	
P(2)	89451.07	89460.12		
Q(1)	112048.28	112057.52	69013.83	69035.81
Q(2)	112064.00	112073.28	68972.45	68994.37
Q(3)	112087.44	112096.72	68910.31	68932.17
Q(4)	112118.40	112127.88	68827.42	68849.20
Q(5)	112156.92	112166.36		
Q(6)	112202.64	112212.12		
R(0)			80365.47	80387.42
R(1)			91735.94	91757.84
R(2)			103144.98	103166.73
R(3)			114591.60	114613.07

[a] Denotes subband type. For the b-type bands the Q-branch transitions terminate on $J'_{K_aK_c}$ levels having $K'_a + K'_c = J'$ and the P- and R-branch transitions terminate on levels having $K'_a + K'_c = J' + 1$. For the c-type bands the Q-branch transitions have $K'_a + K'_c = J' + 1$ and the P- and R-branch transitions have $K'_a + K'_c = J'$.

[b] Symmetry of the rovibronic states involved in the transitions.

TABLE II

Spectroscopic Constants (in MHz) for the $K = 1 \leftarrow 0$ Subbands of DHO–DOD

	b-type[a]		*c*-type	
	$A^{\pm}$	$B^{\pm}$	$A^{\pm}$	$B^{\pm}$
g_I	6	3	6	3
ν_0	117685.182(59)[b]	117694.397(56)	74684.721(16)	74706.7033(59)
$\bar{B}_{K=1}$	5644.620(13)	5644.640(12)	5650.1245(59)	5650.1326(96)
$\bar{B}_{K=0}$	5645.2345[c]	5645.261[c]	5645.2345(53)	5645.261(13)
B-C	17.818(31)	17.897(30)	61.2985(38)	61.259(22)
$D_{K=1}$	0.04334(20)	0.04398(19)	0.04206(28)	0.04265(42)
$D_{K=0}$	0.04176[c]	0.04221[c]	0.04176(30)	0.04221(47)
σ[d]	0.082	0.079	0.019	0.005

[a] Subband type.
[b] One standard error from the fit in units of the last significant digit shown.
[c] Constrained in fit.
[d] Standard deviation of the fit.

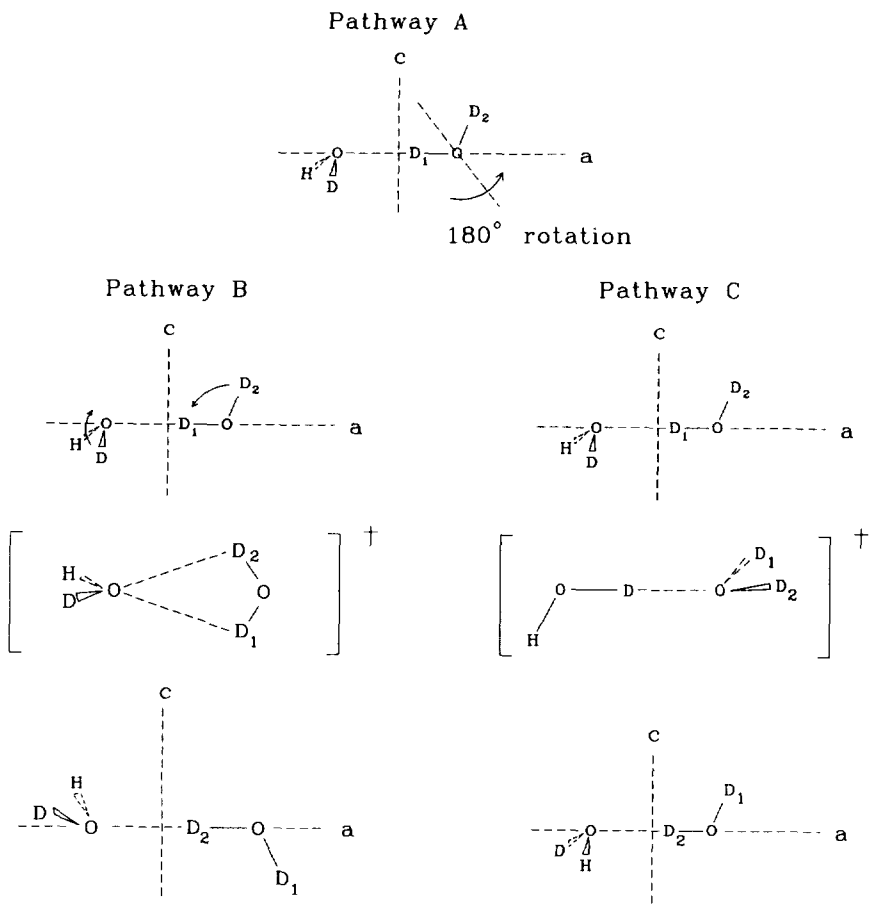

FIG. 3. Three possible tunneling pathways for the deuteron interchange in DHO–DOD.

with pathway C giving rise to most of the 9.2 MHz splitting of the *b*-type band and pathway B giving rise to most of the 22.0-MHz splitting of the *c*-type band.

If tunneling pathway C is indeed significant then this implies that one or both of the two configurations corresponding to the isotopic species D_2O–DOH and D_2O–HOD is sampled during the tunneling processes, with the D_2O–DOH configuration being more likely due to its greater stability compared to D_2O–HOD. These results are reminiscent of the tunneling dynamics of mixed H/D acetylene dimers where a Fermi resonance-type interaction was observed between two isomers of DCCD–DCCH (*10*). Further studies are required on the other $K = 1 \leftarrow 0$ bands of DHO–D_2O to verify the above picture of the tunneling dynamics of DHO–D_2O. It also appears that a more comprehensive investigation of the microwave spectrum of D_2O–DOH is necessary for a complete understanding of the tunneling dynamics in DHO–D_2O. Together, these studies should furnish valuable information on the isotopic dependencies of the tunneling processes in the water dimer to use in modeling the H_2O/H_2O intermolecular potential.

ACKNOWLEDGMENTS

We thank A. A. Ulyanov and O. P. Pavlovsky of NNIPI in Nizhny Novgorod, Russia, for the generous loan of the synthesizer-driven BWO system used in this work.

REFERENCES

1. E. N. KARYAKIN, G. T. FRASER, AND R. D. SUENRAM, *Mol. Phys.* **78,** 1179–1189 (1993).
2. G. T. FRASER, *Int. Rev. Phys. Chem.* **10,** 189–206 (1991); L. H. COUDERT AND J. T. HOUGEN, *J. Mol. Spectrosc.* **139,** 259–277 (1990).
3. J. A. ODUTOLA AND T. R. DYKE, *J. Chem. Phys.* **72,** 5062–5070 (1980).
4. L. H. COUDERT, F. J. LOVAS, R. D. SUENRAM, AND J. T. HOUGEN, *J. Chem. Phys.* **87,** 6290–6299 (1987).
5. G. T. FRASER, R. D. SUENRAM, AND L. H. COUDERT, *J. Chem. Phys.* **90,** 6077–6085 (1989).
6. G. T. FRASER, R. D. SUENRAM, L. H. COUDERT, AND R. S. FRYE, *J. Mol. Spectrosc.* **137,** 244–247 (1989).
7. R. D. SUENRAM, G. T. FRASER, AND F. J. LOVAS, *J. Mol. Spectrosc.* **138,** 440–449 (1989).
8. YU. I. ALEKSHIN, G. M. ALTSHULLER, O. P. PAVLOVSKY, E. N. KARYAKIN, A. F. KRUPNOV, D. G. PAVELIEV, AND A. P. SHKAEV, *Int. J. Infrared Millimeter Waves* **11,** 961–971 (1990).
9. L. H. COUDERT AND J. T. HOUGEN, *J. Mol. Spectrosc.* **139,** 259–277 (1990).
10. K. MATSUMURA, F. J. LOVAS, AND R. D. SUENRAM, *J. Mol. Spectrosc.* **150,** 576–596 (1991).

E. N. KARYAKIN

Molecular Spectroscopy Laboratory
Applied Physics Institute
Nizhnii Novgorod, Russia

G. T. FRASER
B. H. PATE
R. D. SUENRAM

Molecular Physics Division
National Institute of Standards and Technology
Gaithersburg, Maryland 20899
Received April 16, 1993